Original article can be read in Inorganic Chemistry Frontiers, 2021, 8, 1142 - 1153

Indium promoted C(sp^3)-P bond formation by Domino A^3-coupling method - A combined experimental and computational study

Suman Das[a]†, Parveen Rawal[b]†, Jayeeta Bhattacharjee[a]†, Ajitrao Devadkar[a], Kuntal Pal[c], Puneet Gupta,*[b] and Tarun K. Panda*[a]

A highly efficient and green process for the synthesis of α-aminophosphonates has been developed, through a one-pot three-component reaction of various aldehydes, amines, and phosphine oxide in the presence of indium complexes as competent catalysts under the neat condition at room temperature. The indium complexes [κ^2-{RNC(Me)=CHC(Me)=O}$_2$InCl] (R = 2,6-diisopropylphenyl (Dipp), **2a**; 2,4,6-trimethylphenyl (Mes), **2b**), and [κ^2-{DippNC(Me)=CHC(Me)=O}$_2$In(OTf)] [(OTf = $CF_3SO_3^-$, **3a**) were synthesised by the reaction of protic ligand β-ketoimine with equivalent amount of lithium hexamethyldisilazide followed by the addition of indium trichloride in toluene. The solid-state structures of complexes **2a**, **2b**, and **3a** are established by single-crystal x-ray diffraction analysis. In all the indium complexes, the indium ion is five-fold coordinated and adopts a distorted trigonal pyramidal geometry around it. The catalytic method offers an efficient approach with a broad range of α-aminophosphine oxide derivatives in excellent yields with good functional group tolerance. Density functional theory based mechanistic studies demonsrtates energetically affordable pathways at room temperature for the indium catalysed aminophosphorylation of benzaldehyde, phenylamine, and diphenylphosphine oxide. The rate-limiting step deduced in this aminophosphorylation is the initial step in which phenylamine reacts with indium-coordinated benzaldehyde to build a C–N bond with a concomitant transfer of a proton from phenylamine to benzaldehyde.

INTRODUCTION

Organic phosphorus compound such as α-aminophosphonates and related derivatives, considered as the structural analogs of α-amino acids, have significant importance, as ligands in synthetic organic chemistry and mainly in medicinal[1-3], pharmacological and agricultural chemistry[4] due to their potential biological activity such as enzyme inhibitors, antibiotics, antihypertensives, antitumor[5], antibacterial[6], and enzyme-inhibiting properties. Due to this, more efforts have been applied to catalysis research to develop an efficient method for the synthesis of α-aminophosphine oxides over the last years. The two major synthetic routes towards α-aminophosphonate derivatives available in the literature embrace the Kabachnik–Fields (phospha-Mannich) three-component condensation, where an amine, an aldehyde or ketone, and a H-phosphine oxides reagent, such as a dialkyl phosphite or a secondary phosphine oxide react in a one-pot manner [7-9] and also the Pudovik (aza-Pudovik) reaction, in which a H-phosphine oxides species is added on the double bond of imines.[10-11] In both cases, this transformation proceeds via an in situ imine formation, followed by the addition reaction between phosphite nucleophile and imine electrophile to form an N–C–P bond. In most cases, these additions were carried out in the presence of various catalysts and solvents. The use of many types of catalysts, such as Brønsted acids (recent examples are hypophosphorus acid,[12] sulfamic acid[13] and oxalic acid[14] or bases like $CaCl_2$[15] and 1,8-diazabicyclo[5.4.0]undec-7-ene (DBU) [16], tetramethyl guanidine (TMG) [17]metal salts like $Mg(ClO_4)_2$,[18] GaI_2,[19] metal complexes like metal triflates (M(OTf)n, M = Li, Mg, Al, Cu and Ce) [20], bismuth(I) nitrate [21],gallium(III) iodide [22], bismuth(III) chloride [23],lanthanum(III) chloride [24], iron(III) chloride [25], ceric ammonium nitrate (CAN) [26], indium(III) chloride also indium(III) triflate [27] and a variety of lanthanide (Yb, Sm, Sc, La) triflates [28] were well reported in literature. Also, two new viable methods for amino phosphonate synthesis were reported. In the first methodology, various amino phosphonates prepared via carbene insertion of diazo phosphonates into aniline under mild reaction conditions in neat water is described; whereas in the second case, α-aminophosphonates prepared from aryl azides under solvent-free conditions is reported.[29] The enantioselective hydrophosphonylation of imines was also described, where chiral catalysts were applied in various solvents.[30] There are a few examples, where the reactions were performed in a solvent in the absence of any catalyst[31]. As for the microwave (MW)-assisted additions, only two cases were reported, but the catalytic variations were carried out in kitchen MW ovens and thus, do lack of exact temperatures, these results cannot be reproduced.[32,33] Although all the above-mentioned methods have demonstrated their efficiency in the synthesis of α-amino phosphonates, they are also suffering from some drawbacks such as long reaction times and high reaction temperatures, harsh reaction conditions with the use of acids, poor yields, also the use of toxic solvents. Therefore, the development of a milder, convenient, and environmentally benign approach with a broad substrate scope is still under investigation. From a green chemicals' point of view, the solvent-free and catalyst-free additions are of interest, however, in these reactions, relatively long reaction times (1.5 – 10 h), and/or unreasonably large excesses (50–150 equiv) of the dialkyl phosphite were applied.[34,35] The synthesis of α-aryl-α-aminophosphine oxides by the addition of secondary phosphine oxides to imines is much less studied as these reactions cannot be carried out in a one-pot operation with a carbonyl compound, amine, and dialkyl phosphite as the unreacted

amines and water that exist during imine formation can decompose the catalysis present in the reaction medium for further reaction. Only a few publications were found and the reported reactions were performed in the solvent (in DEE, Toluene), [36-37] or in the presence of a chiral catalyst. [38] Owing to the importance of α-aminophosphonates from pharmaceutical, industrial and synthetic points of view, we wished to develop a facile catalyst and solvent-free method for the synthesis of α-aryl-α-aminophosphonates and α-aryl-α-aminophosphine oxides by the addition of dialkyl phosphites or diphenylphosphine oxide to the double bond of imines, and aimed at the preparation of new derivatives.

Scheme 1. Comparison between prior work and current work. In recent years, the use of indium as a catalyst for various organic synthesis has been an ever-growing research area, and a variety of reactions have been developed, such as Diels-Alder reactions,[39-40] epoxide rearrangements,[41] Friedel-Crafts acylations[42], and synthesis of organic molecules. As part of our continuing interest in the development of new synthetic methodologies, we report herein an efficient and convenient procedure for the synthesis of α-aminophosphonates by one-pot three-component reaction of aldehyde, amine and diethyl phosphite catalyzed by β-ketoiminato indium complexes under solvent-free conditions.

Result and Discussion

Synthesis of β-ketoiminato Indium (III) Complexes:

The bis-β-ketoiminato indium (III) complexes [In(Cl)(RNHC(Me)= CHC(Me)O)$_2$] (R = Dipp, Mes, **2a**, **2b**) were synthesized in good yield through a one-pot reaction using β-ketoimine **1a** and **1b** as protonic ligands with an equivalent amount of lithium hexamethyldisilazide in

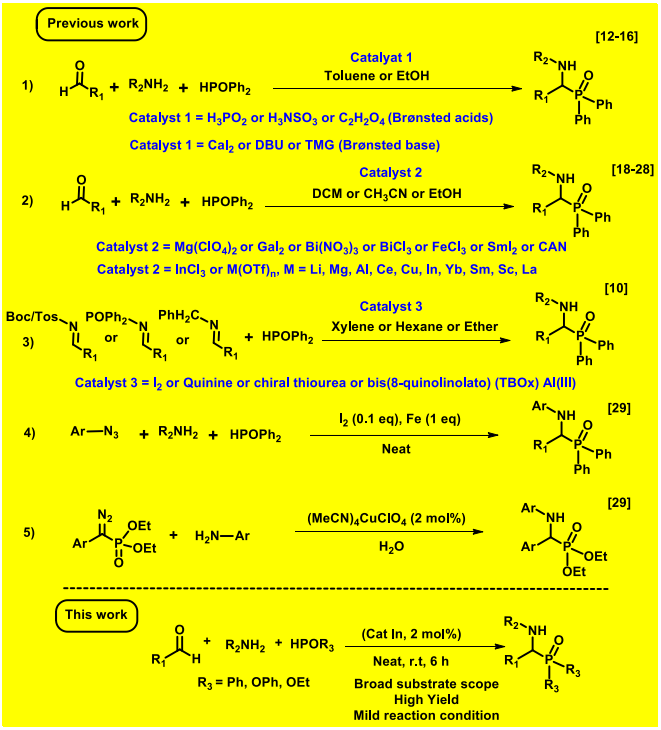

room temperature followed by addition of indium trichloride(III) in 2:2:1 molar ratio for 12 hours in toluene (Scheme 2). Further reaction of Indium complexes **2a** with AgOTf at room temperature in toluene afforded the corresponding bis-β-ketoiminato Indium (III) triflate complexes [In(OTf)(RNHC(Me)= CHC(Me)O)$_2$] (R = Dipp, **3a**) in very good yield (Scheme 2). All the new indium complexes **2a**, **2b**, and **3a** were showed good solubility in a common organic solvent such as THF, toluene, diethyl ether, and all the air and moisture sensitive complexes **2a,b** and **3a** were characterized by using standard spectroscopic and analytical techniques. The solid-state structures of complexes **2a**, **2b,** and **3a** were established by single-crystal x-ray diffraction analysis.

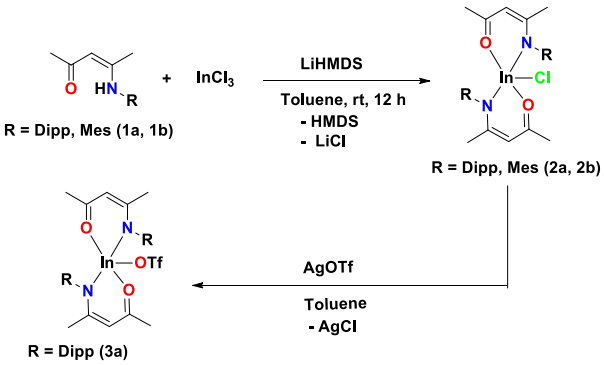

Scheme 2. Synthesis of indium complexes (**2a,b** and **3a**).

In the ^{1}H NMR spectra, a characteristic singlet resonance signal at δ_H 4.63 ppm (for **2a**), 4.92 ppm (for **2b**), and 4.64 ppm (for **3a**) was observed for the corresponding enamine (N-C=CH) proton of the β-ketoiminato ligand backbone. The resonance signals for the CH_3 protons attached to the β-ketoiminato ligand backbone appeared as a singlet at δ_H 1.31, 1.25 (for **2a**), and at δ_H 2.15, 1.99 ppm (for **2b**). For complexes, **2a** and **3a**, two sets of septets signals centered at δ_H 3.45 and 3.04 ppm (for **2a**) and δ_H 3.46 and 3.04 ppm (for **3a**) were observed due to the methine protons (-CH) present in the 2,6-diisopropylphenyl fragments. Additionally, four doublets were also obtained for complexes, **2a** and **3a**, due to methyl (CH_3) hydrogen atoms present in the Dipp fragments (see FS1, FS3, FS5 in ESI). In the $^{13}C\{^1H\}$ NMR spectra, resonance signals for the corresponding carbonyl carbon (C=O) 186.6 (for **2a** and **3a**), 186.3 (for **2b**), and imine carbon (N=CH) δ_C and 177.4 ppm (for **2a** and **3a**), 173.1 (for **2b**) were observed which are significantly low-field shifted when compared to the free ligand **1a**,**b** (see FS2, FS4, FS7 in ESI).

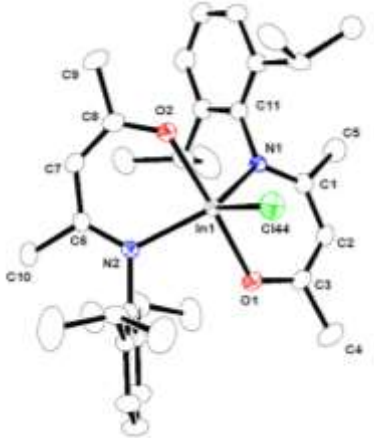

Fig. 1 ORTEP drawing of the molecular structures of indium complex **2a**; ellipsoids are drawn to encompass 30% probability. Hydrogen atoms are omitted for clarity. Selected bond lengths (Å) and angles (deg) are given. Some hydrogen atoms are omitted for clarity: In1–O1 2.105(2), In1–O2 2.103(2), In1–N1 2.186(2), In1–N2 2.189(3), In1–Cl44 2.376(10), O1–C3 1.285 (4), O2–C8 1.283(4), N1–C1 1.321(4), N2–C6 1.325(4), C1–C2 1.408(4), C2–C3 1.363(5), C6–C7 1.409(5), C7–C8 1.362(5), O2–In1–O1 172.09(10), O2–In1–N1 89.81(9), O1–In1–N1 86.88(9), O2–In1–N2 86.45(9), O1–In1–N2 89.90(9), N1–In1–N2 127.81(9), O2–In1–Cl44 95.76(7), O1–In1–Cl(44) 92.09(7), N1–In1–Cl44 107.96(7), N2–In1–Cl44 124.21(7), C3–O1–In1 122.1(2), C8–O2–In1 128.2(2), C1–N1–C11 119.2(3), C1–N1–In1 121.5(2), C(11)–N(1)–In(1) 118.9(2), C(6)–N(2)–C(23) 118.8(3), C(6)–N2–In1 124.1(2), C23–N2–In1 117.06(18). CCDC 2035015.

Fig. 2 ORTEP drawing of the molecular structures of indium complex **2b**; ellipsoids are drawn to encompass 30% probability. Hydrogen atoms are omitted for clarity. Selected bond lengths (Å) and angles (deg) are given. Some hydrogen atoms are omitted for clarity: In1–O1 2.077(6), In1–O2 2.086(7), In1–N1 2.169(7), In1–N2 2.184(8), In(1)–Cl44 2.382(2), O1-C3 1.313(10), O2-C8 1.334(12), N1-C1 1.324(11), N2-C6 1.353(12), C6-C7 1.384(14), C7-C8 1.392(14), O1–In1–O2 171.8(2), O1–In1–N1 87.9(3), O2–In1–N1 90.0(3), O1–In1–N2 88.8(3), O2–In1–N2 86.0(3), N1–In1–N2 125.3(3), O1–In1–Cl44 95.54(17), O2–In1–Cl44 92.48(19), N1–In1–Cl44 116.93(19), N2–In1–Cl44 117.65(19), C3–O1–In1 129.8(6) C8–O2–In1 128.0(6), C1–N1–C11 118.5(7), C1–N1–In1 124.6(6), C11–N1–In1 116.8(5), C6–N2–In1, 125.7(6), C20–N2–In1 115.6(6). CCDC 2035016.

The attachment of the β-ketoiminato ligands to the indium ion was confirmed by establishing the molecular structures of complexes **2a**, **2b,** and **3a** in their solid-state by single-crystal x-ray diffraction analysis. The indium chloride complexes **2a** and **2b** crystallize in the monoclinic space groups C2/c and $P2_1/c$, respectively with two independent molecules in the unit cell. The molecular structures of complexes **2a** and **2b** are shown in Figures 1 and 2 respectively. The details of the structural and refinement parameters are given in Table TS1 in supporting information. The five-fold coordination number is observed for both the complexes **2a** and **2b** by the κ^2-chelation mode of two β-ketoiminato ligands and one chloride ions to the central indium ion adopting a distorted bipyramidal geometry with geometric parameter τ = 0.77 (**2a**), 0.74 (**2b**) in each case. In both the complexes, distorted bipyramidal geometry is formed by the chelation of two nitrogen atoms N1 and N2 of the β-ketoiminato ligands and one chloride ion (Cl 44) in the equatorial position and two oxygen atoms O1 and O2 in the apical position in each case. The indium nitrogen bond distances of 2.169(7), 2.184(8) Å (for **2a**), 2.186(2), 2.189(3) Å (for **2b**) are similar and have an indication of indium amido bond and are in agreement with reported Indium amido complexes.[43] The indium oxygen bond distances of 2.077(6), 2.086(7) Å (for **2a**), 2.105(2), 2.103(2) Å (for **2b**) are relatively shorter than In-N bonds indicating the presence of delocalization of electron density to the nitrogen and oxygen centres of the ligand backbone. The indium chlorine distance of 2.382(2) Å (2a) and 2.3762(10) Å are quite similar and are slightly longer than those found in $InCl_3$. Two six-membered metallacycles In1-N1-C1-C2-C3-O1 and In1-N2-C6-C7-C8-O2 (for **2a** and **2b**) are formed in each case and a dihedral angle of 62 º (2a) and 46.5º (2b) are also observed between the two six-membered mean planes.

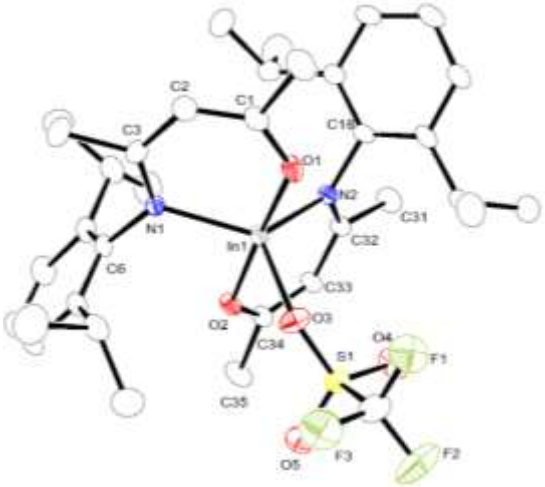

Fig. 3
ORTEP drawing of the molecular structures of indium complex **3a**; ellipsoids are drawn to encompass 30% probability. Hydrogen atoms are omitted for clarity. Selected bond lengths (Å) and angles (deg) are given. Some hydrogen atoms are omitted for clarity. In1–O2 2.070(3), In1–O1 2.076(3), In1–N2 2.147(3), In1–O3 2.153(3), In1–N1 2.159(3), O2–In1–O1 174.61(13), O2–In1–N2 90.50(12), O1–In1–N2 92.60(13), O2–In1–O3 88.24(13), O1–In1–O3 86.42(14), N2–In1–O3 117.68(14), O2–In1–N1 92.99(12), O1–In1–N1 88.40(12), N2–In1–N1 129.91(13), O3–In1–N1 112.37(14). CCDC 2035020.

The bis-β-ketoiminato indium (III) triflate complex [In(OTf)(DippNHC(Me)=CHC(Me)O)$_2$], **3a** crystallizes in the triclinic space group *P*-1. The molecular structure of complex **3a** in solid-state is shown in Figures 3, and details of the structural parameters are given in Table TS 1 in supporting information. Similar to complexes 2a and 2b, the two β-ketoiminato ligands are attached to the indium ion in complex 3 through donor nitrogen and oxygen atoms of each ligand in a κ^2-chelating fashion through *trans* coordination. Additionally, the centre indium ion is attached with an oxygen atom of the triflate (OTf) group to make the metal ion fivefold coordinated. The geometry around the indium ion can best be described as distorted trigonal bipyramidal with me geometric parameter τ = 0.74. Two oxygen atoms O1 and O2 occupy the apical position whereas N1, N2, and O3 occupy the equatorial position of the trigonal bipyramid. The indium nitrogen distances of 2.159(3) and 2.147(3) Å are similar

to those observed in complexes **2a** and **2b**. The indium oxygen bond distances In1-O1 2.076(3) and In1-O2 2.070(3) Å are much shorter than In1-O3 2.153(3) due to the preferential less sterically crowded apical position of O1 and O2 compare to an equatorial position of the O3 atoms of sterically bulky triflate group. Two six-membered metallcycles In1-O1-C1-C2-C3-n1 and In1-N2-C32-C33-C34 are formed due to κ^2-coordination of the monoanionic β-ketoiminato ligands and a dihedral angle of 50º is observed between the mean planes of two six-membered rings.

Catalysis reaction for C-P bond formation by using indium catalyst:

All three indium complex **2a**, **2b**, and **3a** were first tested as precatalysts for aminophosphorylation of aldehyde, amine and phosphine oxide to make corresponding aminophosphinated product. Representative results are given in Table 1.

In the beginning, catalytic experiments were performed using 2 mol % of the indium complex (i.e. **2a**, **2b** or **3a**) along with equimolar amounts of benzaldehyde, aniline, and phosphine oxide under the neat condition at room temperature for six hours. We are delighted to observe that all the catalysts **2a**, **2b** and **3a** exhibited significant catalytic activity for the same reaction and resulted in the formation of the corresponding aminophosphinated product in excellent yield 81-97% (Table 1, entries 1-3). As a control experiment, aminophosphorilation of aldehyde, amine with phosphine oxide was performed in the absence of the catalyst, it did not yield any product at room temperature as well as at elevated temperature (Table 1, entry 4). Table 1 also shows that the reaction has no notable effect on the product formation by an increase of temperature or the reaction time as there was no enhancement in yield at high temperature and longer reaction time whereas lowering the reaction time, the yield of the reaction decreases (Table 1, Entry 5 and 6). Additionally, when the aminophosphorylation of aldehyde, amine, and phosphine oxide was performed using a higher equivalent of phosphine oxide, almost a similar yield of α-aminophosphonate was obtained (Table 1, entries 7) indicating no remarkable impact on the efficiency of the reaction. We also have studied the effect of various solvents such as hexane, toluene, and THF for the formation of aminophosphinated product (Table 1, Entries 8-10). It was observed that the lower yield of ~81% of the product obtained in the presence of a solvent. Thus using 2 mol % of the indium complex **3a** under the neat condition at room temperature and 6 hours of reaction time were chosen as optimal conditions for the catalytic aminophosphorylation of aldehyde, amine, and phosphine oxide.

Table 1. Screening of Indium complexes as a pre-catalyst for aminophosphorylation of aldehyde, amine, and phosphine oxide to yield the corresponding aminophosphinated product.

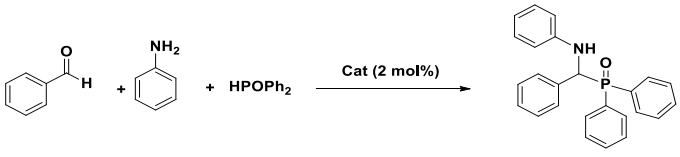

S.No	Catalyst	phosphine oxide (equiv)	Solvent	Temp (° C)	Time (h)	% yield[a]
1.	**2a**	1	Neat	r.t.	6	82
2.	**2b**	1	Neat	r.t.	6	89
3.	**3a**	1	Neat	r.t.	6	97
4.	**None**	1	Neat	r.t. and 90	12	0
5.	**3a**	1	Neat	90	24	97
6.	**3a**	1	Neat	r.t.	2	71
7.	**3a**	1.5	Neat	r.t.	6	96
8.	**3a**	1	Hexane	r.t.	12	86
9.	**3a**	1	Toluene	r.t.	12	83
10.	**3a**	1	THF	r.t.	12	81

All the reaction was performed with benzaldehyde (1.0 mmol), aniline(1.0 mmol) and triethyl phosphate (1.0 mmol) in neat condition at room temperature. [a]Isolated yield.

In a further study with the optimized conditions established, the scope and generality of this reaction were investigated by reacting varieties of aldehydes, amines, and diphenylphosphine oxide in using 2 mol % of the indium complex **3a** under the neat condition at room temperature for 6 hours. The respective α-aminophosphonates derivatives were isolated in each case and analyzed through ^{1}H and ^{13}C, ^{31}P NMR spectroscopy (see ESI). The yields were calculated after the isolation of pure products. The reactions displayed a broad substrate scope. The results of the catalytic reaction are presented in Table 2. It was found that the benzaldehyde having both electron-donating (methyl, methoxy, amido) and withdrawing group (such as fluro, chloro, nitro, cyano) is well tolerated to furnish corresponding products in excellent yields (Table 2, entry 4b-4m). Besides, the steric influence of the substituents of benzaldehyde was also worked well in this reaction to deliver the products 4 h in good yield. Notably, anilines with both electron-rich and deficient groups on the aryl ring proceeded smoothly and offered the respective products in high yield (Table 2, entry 4n-4r). The aminophosphorylation reaction was also worked smoothly using anilines with bulkier substituents on the phenyl ring such as diphenylmethanamine, 2,6-dimethylaniline, leading to the desired product in high yield (Table 2, entry 4p and 4r). These results demonstrate that this protocol provided an efficient, facile, and practical method for the synthesis of α-aminophosphonates under ambient conditions.

Table 2. Scope of bis-β-ketoiminate Indium (III) complex **3a** catalyzed synthesis of α-aminophosphonates.

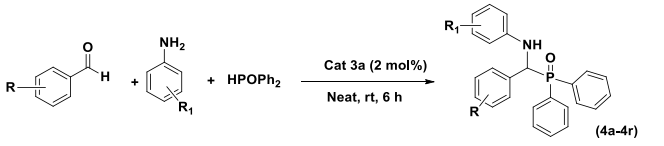

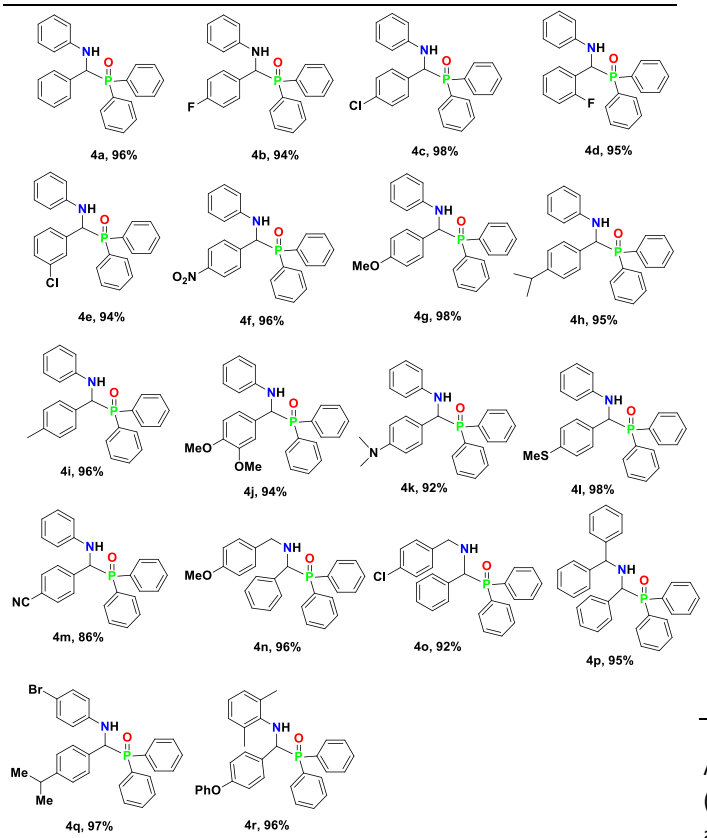

All reaction was performed with benzaldehyde (1.0 mmol), aniline (1.0 mmol), diphenylphosphine oxide (1.0 mmol), and complex **3a** (18 mg, 0.02358 mmol, 2 mol%) in neat condition at room temperature for 6 hours. Yields were calculated as an isolated yield basis.

The substrate scope was further expanded to diethyl phosphonate and diphenyl phosphonate. The reaction of diethyl phosphonate and diphenyl phosphonate with varieties of substituted aldehydes, amines, having o-/p-Me, methoxy group, alkyl groups, halides, and amide proceeded very smoothly and resulted in the selective production of the corresponding α-aminophosphonates derivatives with ~82-96% yield (Table 3, 5a-5g and 6a-6j). The molecular structure of 4m, 6b, and 6d is shown in Figures 4, 5, and Figure 6. From this survey, we see that complex **3a** displayed a broad substrate scope.

Table 3. Scope of bis-β-ketoiminate indium (III) complex **3a** catalyzed synthesis of α-aminophosphonates.

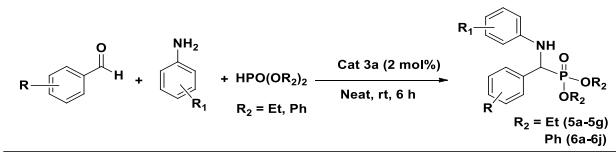

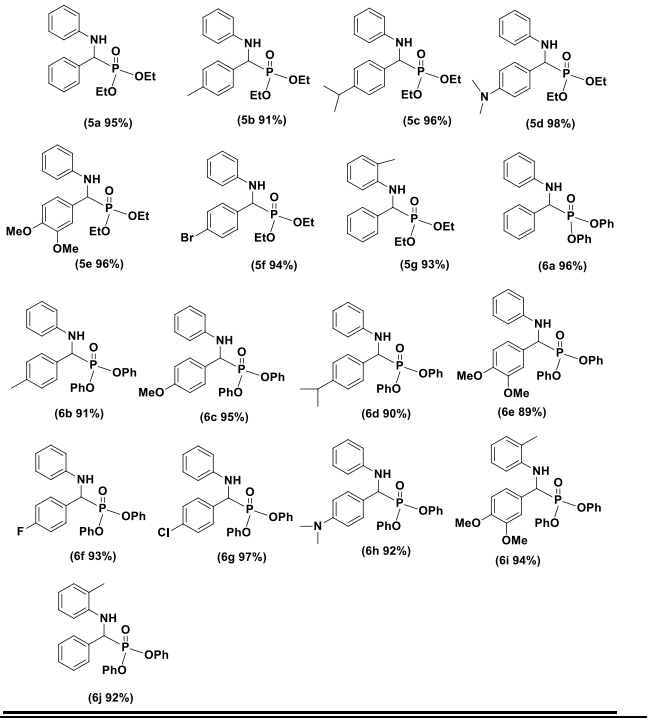

All reaction was performed with benzaldehyde (1.0 mmol), aniline (1.0 mmol), diethyl phosphonate/diphenyl phosphonate (1.0 mmol), and complex **3a** (18 mg, 0.02358 mmol, 2 mol%) in neat condition at room temperature for 6 hours. Yields were calculated as an isolated yield basis.

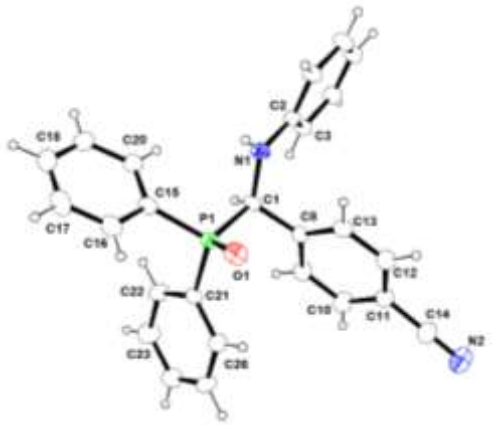

Fig. 4 The solid-state structure of diphenyl ((phenylamino)(p-tolyl)methyl)phosphonate **4m**. Some hydrogen atoms are omitted for clarity. Selected bond lengths (Å) and bond angles (°): P1–O1 1.4789(15), P1–C1 1.8417(19), P1–C21 1.795(2), P1–C15 1.792(2), C1–N1 1.444(2), P1–C1–N1 110.12(12), C1–P1–O1 112.30(9). CCDC 2035017.

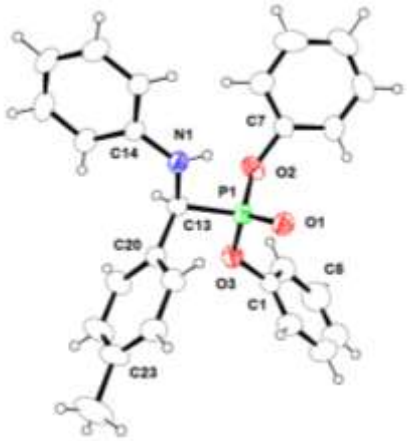

Fig. 5 The solid-state structure of diphenyl ((phenylamino)(p-tolyl)methyl)phosphonate **6b**. Some hydrogen atoms are omitted for clarity. Selected bond lengths (Å) and bond angles (°): P1–O1 1.449(3), P1–O2 1.576(3), P1–O3 1.570(3), P1–C13 1.817(4), C13–N1 1.452(5), P1–C13–N1 106.9(3), C13–P1–O1 116.58(18), C13–P1–O2 106.52(18), C13–P1–O3 99.56(17), O1–P1–O3 116.80(17), O1-P1–O2 114.49(18), O3–P1–O2 100.70(17). CCDC 2035019.

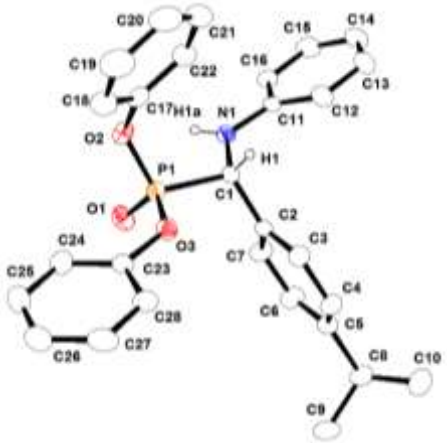

Fig. 6 The solid-state structure of diphenyl ((phenylamino)(p-tolyl)methyl)phosphonate **6d**. Some hydrogen atoms are omitted for clarity. Selected bond lengths (Å) and bond angles (°): P1–O1 1.454(3), P1–O2 1.584(3), P1–O3 1.580(3), P1–C1 1.824(3), C1–N1 1.461(4), P1–C1–N1 106.3(2), C1–P1–O1 115.18(17), C1–P1–O2 109.31(15), C1–P1–O3 99.65(14), O1–P1-O3 117.09(16), O1–P1–O2 109.06(16), O3–P1–O2 105.83(14). CCDC 2035018.

To the best of our knowledge, **3a** is the first example of β-ketoiminato indium complex as a competent catalyst for the one-pot synthesis of α-aminophosphonates under solvent-free condition, room temperature, low catalyst loading, and reduced reaction time to give excellent yield with broader substrate scope and high functional group tolerance compared to the other indium precatalysts reported in the literature.[27]

Most plausible mechanism

The most plausible mechanistic pathway for the aminophosphorylation of aldehyde, amine, and phosphine oxide to yield the corresponding aminophosphinated product by indium(III) precatalyst **3a** is depicted in Scheme 3. In the initial step of this stepwise process, the indium precatalyst **3a** reacted with one equivalent of aldehyde. The nucleophilic attack of the nitrogen atom from the incoming arylamine onto the electrophilic carbon center resulted in the formation of the intermediate imine complex (**I**) upon the elimination of H_2O. Complex (**I**), the active catalyst, further reacted with one equivalent of phosphine oxide to give a tetrahedral zwitterionic intermediate (**II**). In the final step, the active, β-ketoiminate indium triflate species are regenerated by eliminating the corresponding free α-aminophosphonates product.

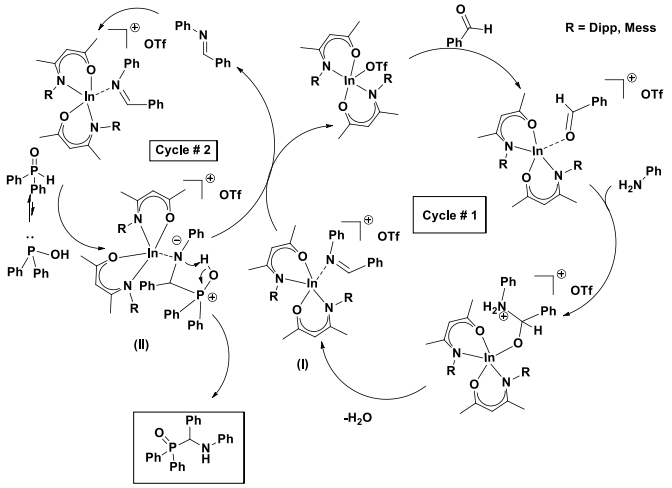

Scheme 3. A most plausible mechanism for the aminophosphorilation of aldehyde, amine, and phosphine oxide to yield the corresponding aminophosphinated product by indium(III) precatalyst **3a**.

Computational Study

Computational Model System and Computational Details: It is proposed in Scheme 2 that in the initial steps of the reaction the indium catalyst reacts with benzaldehyde and phenylamine. So, to perform DFT calculations we built a computational model consists of the indium catalyst, benzaldehyde and phenylamine (Fig. 7). In the model system, small methyl groups are considered in place of large 2,6-diisopropylphenyl (dipp) and 2,4,6-trimethylphenyl (mes) groups to save computational time and resources. DFT calculations were carried out using the ORCA4.2 quantum chemical program package.[44] The relative Gibbs free energies reported in mechanistic studies were obtained at the BP86[45,46]-D3[47]/def2-TZVP[48] // BP86-D3/def2-SVP[48] level of DFT. Refer to the supporting information for computational details. All Gibbs free energies reported in mechanistic studies are in kcal mol^{-1} and relative to **A** (computational model).

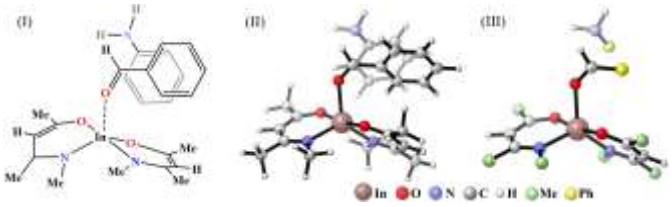

Fig. 7 (I) Schematic representation of the computational model (**A**) for DFT calculations. (II) 3-D view of the model **A**. (III) The unclouded 3-D view of the model **A**. Note that the phenyl rings (Ph) and methyl groups (Me) are considered in all DFT calculations.

DFT based Mechanistic Studies

(i) Indium Catalyzed Condensation of Benzaldehyde with Aniline: We commence our mechanistic studies using the computational model shown in Fig. 7 in which benzaldehyde is coordinated to the indium-center at the axial position and aniline is π-stacked with benzaldehyde. In the first step (**A**→**TS$_{AB}$**, Fig. 8**)**, phenylamine reacts with the indium-coordinated benzaldehyde to form a C–N σ-bond between the electrophilic carbonyl carbon of benzaldehyde and nucleophilic nitrogen of phenylamine with a concomitant transfer of a proton from the nitrogen of phenylamine to the oxygen of benzaldehyde. The transition state **TS$_{AB}$** with an activation barrier of 22.6 kcal mol^{-1} leads to a carbinolamine intermediate **B** (ΔG_{298} = 7.4 kcal mol^{-1}). It is evident that **A**→**B** is reversible as **B** is less stable compared to **A**. To illustrate the orbital interactions in the first step, selected quasi-restricted orbitals (QROs)[49] are plotted in Fig. 9. QROs show the formation of the σ(N–C) bond and the proton transfer steps.

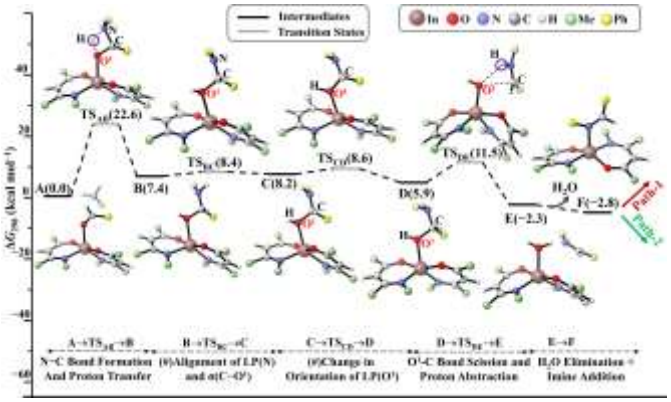

Fig. 8 DFT derived mechanistic pathway for indium catalyzed condensation of benzaldehyde with phenyl amine. DFT method used in the study is BP86-D3/def2-TZVP // BP86-D3/def2-SVP. Gibbs free energies ΔG_{298} [kcal mol^{-1}] are relative to **A**. (#: Refer to Fig. 10 for QROs studies of **B**→**TS$_{BC}$**→**C** and **C**→**TS$_{CD}$**→**D**)

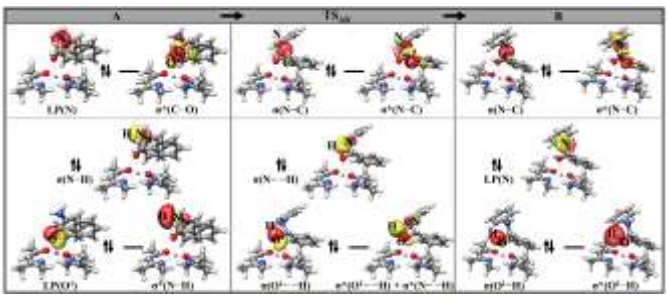

Fig. 9 QROs are plotted for **A**, **TS$_{AB}$** and **B**. Here, **LP** is lone pair. QROs in the first row illustrate the formation of the σ(**N–C)** bond between phenylamine and benzaldehyde. QROs in the second row display the proton transfer from N (of phenylamine) to O^1 (of benzaldehyde).

Subsequent to **A**→**TS$_{AB}$**→**B**, we expected **B** to undergo a second proton transfer to yield an imine intermediate. However, to our surprise, we could not locate a transition state for the second proton transfer from **B**. To understand the reason behind this failure, we plotted relevant QROs of **B**. The QROs under discussion are illustrated in the first row of Fig. 10. It is noticed that in **B** the lone pair present on nitrogen is not properly aligned with the σ(O^1–C) orbital, whereas **B**→**TS$_{BC}$**→**C** conversion brings them into one plane. The successive **C**→**TS$_{CD}$**→**D** step orients the oxygen (O^1) lone pair away from the nitrogen-centered lone pair to reduce the repulsion (Fig. 10, second row). So, the intermediate **D** is more stable than **C**. The conversions **B**→**TS$_{BC}$**→**C** and **C**→**TS$_{CD}$**→**D** can be achieved via minute activation barriers and the reaction steps **B**→**C** and **C**→**D** construct a flat energy plot (Fig. 8).

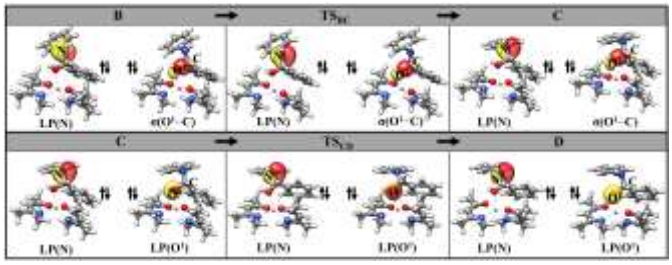

Fig. 10 Here, **LP** is lone pair. The first-row QROs illustrate an alignment arising between **LP**(N) and the σ(O^1–C) orbitals. The second-row QROs display a rotation of the oxygen-centered lone pair around the C–O^1 bond axis to reduce the repulsion between **LP**(N) and **LP**(O^1).

D undergoes a σ(C–O^1) bond scission to result an imine π(N–C) bond and a lone pair on oxygen (O^1) in **TS$_{DE}$** (Figs. 8 and 11). The **LP**(O^1) abstracts a proton to form a σ(O^1–H) bond in **E**. The σ(C–O^1) bond scission and the proton abstraction steps proceed via a concerted mechanism. The activation barrier for **D**→**TS$_{DE}$**→**E** is only 5.6 kcal mol^{-1} and **E** is more stable than its all the preceding intermediates thus the formation of **E** would drive the reaction in the forward direction. The axially-coordinated water in **E** easily eliminates to yield an imine-coordinated complex **F**. Two probable pathways branch off from **F** at this point.

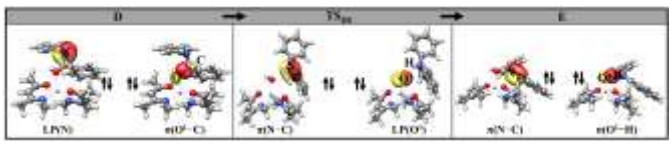

Fig. 11 Here, **LP** is lone pair. QROs illustrate the formation of a π(N–C) bond in imine and a σ(O^1–H) bond in axially-coordinated water in **E**.

(ii) Phosphorylation of Imine Complex of Indium:

Path-1: Diphenyl phosphine oxide ((Ph)$_2$P(=O)H) with **F** produce a stable adduct **G'** (ΔG_{298} = −7.3 kcal mol^{-1}, relative to **A**, Fig. 12) which undergoes a proton transfer and a σ(P–C) bond formation in a

concerted way to yield the product **H'** (ΔG_{298} = −26.3 kcal mol^{-1}, relative to **A**, Fig. 12) via a transition state $\mathbf{TS_{G'H'}}$. The activation barrier for this conversion is 54.1 kcal mol^{-1} which is too high to access at room temperature. Thus, the path-1 can be discarded.

Path-2: An alternate mechanism for the phosphorylation of **F** is explored (Fig. 13). In place of diphenyl phosphine oxide ($(Ph)_2P(=O)H$) its tautomerized species $(Ph)_2P–OH$ reacts with **F** to form a stable adduct **G**. Detailed study on $(Ph)_2P(=O)H \rightarrow (Ph)_2P–OH$ tautomerization is provided in ESI. The intermediate **G** readily undergoes nucleophilic attack by $(Ph)_2P–OH$ to the electrophilic carbon (of imine) via a flat transition state $\mathbf{TS_{GH}}$ which results in the formation of a σ(P−C) bond in the intermediate **H** (ΔG_{298} = −17.4 kcal mol^{-1}, relative to **A**) (Fig. 13 and Fig. 14, first row). Subsequently, the lone pair residing on nitrogen in **H** readily abstract a proton to form a σ(N−H) bond in **I** via a transition state $\mathbf{TS_{HI}}$ (Fig. 13 and Fig. 14, second row). **I** is the most stable species in the overall energy profile and hence the formation of **I** would drive the reaction forward. Moreover, the minute transition state barriers throughout the reaction profile suggest path-2 to be preferred over path-1 for the phosphorylation of the imine complex of indium (**F**). Hence, the proposed indium catalyst is found to be efficient for the aminophosphorylation of benzaldehyde, aniline and diphenylphosphine oxide.

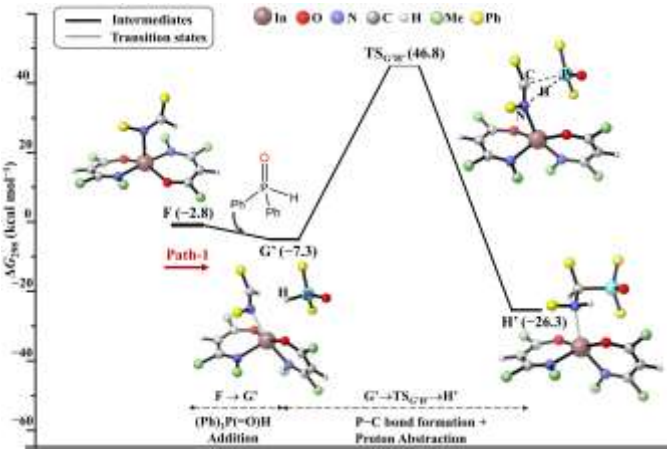

Fig. 12 DFT derived mechanistic pathway for the indium catalyzed phosphorylation of the imine complex (**F**). DFT method used in the study is BP86-D3/def2-TZVP // BP86-D3/def2-SVP. Gibbs free energies ΔG_{298} [kcal mol^{-1}] are relative to **A** (shown in Fig 8).

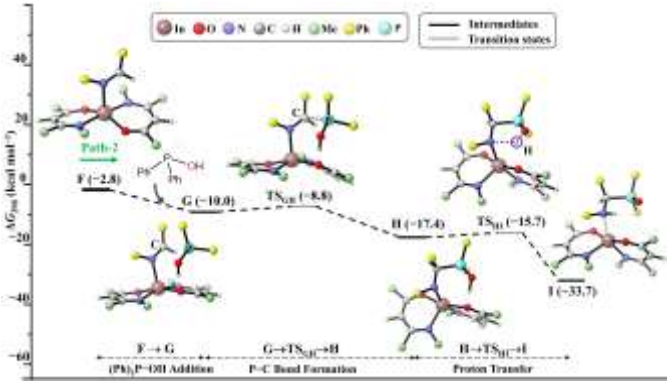

Fig. 13 DFT derived mechanistic pathway for the indium catalyzed phosphorylation of the imine complex (**F**). DFT method used in the study is BP86-D3/def2-TZVP // BP86-D3/def2-SVP. Gibbs free energies ΔG_{298} [kcal mol^{-1}] are relative to **A** (shown in Fig 8).

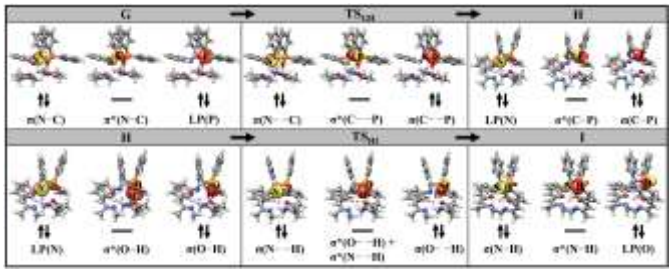

Fig. 14 Here **LP** is lone pair. The first-row QROs illustrate the formation of a σ(P−C) bond in $\mathbf{G \rightarrow TS_{GH} \rightarrow H}$. The second-row QROs display a proton abstraction in $\mathbf{H \rightarrow TS_{HI} \rightarrow I}$ by the nitrogen lone pair to make a σ(N−H) bond in **I**.

Conclusions

In summary, we successfully have prepared a series of new indium metal complexes **2a**, **2b,** and **3a** supported by the bulky β-ketoimine ligands. The structures of the heteroleptic indium complexes **2a**, **2b,** and **3a** were confirmed using X-ray crystallography. In the solid-state, for all three complexes, the monoanionic β-ketoiminato exhibited κ^2 -chelation mode to adopt a distorted tetragonal bipyramidal geometry around the indium ion. The indium triflate complexes **3a** was used as an active pre-catalyst for the one-pot three-component reaction for the synthesis of α-amino phosphonates through the reaction of aldehydes, amines with phosphine oxide. The method allows operational simplicity and mild reaction conditions for the preparation of a wide variety of α-aminophosphonates which is tolerant to a variety of sensitive functional groups, given a very high yield. Detailed DFT investigations for the indium catalyzed aminophosphorylation of benzaldehyde, phenylamine and diphenylphosphine oxide were performed in two parts: (i) indium catalyzed condensation of benzaldehyde with phenylamine, and (ii) indium catalyzed phosphorylation of the imine complex. DFT showed that the rate-determining step has an activation barrier of ~23 kcal mol^{-1} and other activation barriers involved in the mechanistic pathways were below 10 kcal mol^{-1}. Thus, indeed this indium catalyzed aminophosphorylation is easily achievable at room temperature. Quasi restricted orbital analysis has pinpointed all the key orbital overlaps occurred in the course of reactions.

Experimental

General: All manipulations of air-sensitive materials were performed with the rigorous exclusion of oxygen and moisture in flame-dried Schlenk-type glassware either on a dual manifold Schlenk line, interfaced to a high vacuum (10^{-4} torr) line or in an argon-filled M. Braun glove box. Hydrocarbon solvents (toluene and *n*-pentane) were distilled under nitrogen from $LiAlH_4$ and stored in the glove box. ^{1}H NMR (400 MHz) and $^{13}C\{^1H\}$ NMR (100 MHz) spectra were

recorded on a BRUKER AVANCE III-400 spectrometer. BRUKER ALPHA FT-IR was used for FT-IR measurement. Elemental analyses were performed on a BRUKER EURO EA at the Indian Institute of Technology Hyderabad. β-ketoimine ligands **1a** and **1b** and all the amides were synthesized according to the published procedure.[50] The NMR solvent C_6D_6 was purchased from Sigma Aldrich. Crystallographic data for the structures reported in this paper have been deposited with the Cambridge Crystallographic Data Centre as supplementary publication no. CCDC 2035015 (**2a**), CCDC 2035016 (**2b**), CCDC 2035020 (**3a**), CCDC 2035017 (**4m**), CCDC 2035019 (**6b**), CCDC 2035018 (**6d**).

Preparation of [{(DippNC(Me)=CHC(Me)=O}$_2$InCl] (2a) : In a dry 25 mL Schlenk flask, β-ketimine ligand **1a** [R = Dipp; (200 mg, 0.6920 mmol), 5 mL of toluene was placed, to this solution, a mixture of lithium bis(trimethylsilyl)amide (58 mg, 0.3460 mmol) was added and the resulting reaction mixture was kept under stirring at room temperature for 6 hours. Then a solution of indium trichloride (76 mg, 0.340 mmol)and 5 mL of toluene was added onto reaction mixture, kept under stirring for overnight at room temperature. A white precipitate was observed which was filtered off and the filtrate was evaporated under *vacuum* to give a colourless residue. The residue was washed with dry *n*-pentane (5 mL). The compound **2a** was re-crystallised from toluene at –35 °C, and colorless crystals were obtained after 3 days.

Yield: 392 mg, 85%. ^{1}H NMR (400 MHz, C_6D_6, 25 °C): δ_H 7.08 – 7.01 (m, 4H, Ar), 6.95 – 6.90 (m, 2H, Ar), 4.63 (s, 2H, NC*H*), 3.50 – 3.43 (m, 1H, C*H*), 3.07 – 3.00 (m, 1H, C*H*), 1.51 (s, 3H, CH_3), 1.31 (s, 3H, CH_3), 1.25 (s, 3H, CH_3), 1.14 – 1.13 (d, 3H, (CH_3)$_2$), 1.05 – 1.02 (d, 3H, (CH_3)$_2$) ppm. ^{13}C{^{1}H} NMR (100 MHz, C_6D_6): δ_C 186.6, 177.4, 143.5, 143.0, 141.6, 129.1, 128.4, 127.9,127.6, 126.4, 125.5, 124.4,123.0, 97.2, 28.7, 28.4, 26.8,25.0,24.6,24.4,23.8,22.4. ppm. Elemental analysis: $C_{34}H_{48}ClInN_2O_2$ (667.0): calcd C 61.22, H 7.25, N 4.20. Found C 60.87, H 7.09, N 4.13.

Preparation of [In(Mes(NHC(Me)=CHC(Me)O$_2$)Cl] (2b) : The complex **2b** was obtained by similar procedure of complex **2a** by using β-ketimine ligand **1b**. The complex **2b** was re-crystallised from toluene at –35 ºC, and colourless crystals were obtained after 2 days.

Yield: 471.6 mg, 88%. ^{1}H NMR (400 MHz, C_6D_6, 25 °C): δ_H 6.73 – 6.67 (s, 4H, Ar), 4.92 (s, 2H, NC*H*), 2.40 (s, 3H, CH_3), 2.15 (s, 3H, CH_3), 1.99 (s,3H, CH_3) 1.14 – 1.13 (s, 6H, CH_3) ppm. ^{13}C{^{1}H} NMR (100 MHz, C_6D_6): δ_C 186.6, 173.0, 144.5, 134.0, 131.9, 131.1, 131.8, 129.4, 129.1, 129.0, 128.2, 128.0,127.9, 96.5, 27.9, 21.9, 21.9, 20.8, 18.5, 17.3. ppm. Elemental analysis: $C_{56}H_{72}Cl_2In_2N_4O_4$ (1165.7): calcd C 57.70, H 6.23, N 4.81. Found C 57.57, H 6.19, N 4.69.

Preparation of [In (DippNHC(Me)=CHC(Me)O$_2$)OTf] (3a): In a dry 25 mL Schlenk flask, **1a** (200 mg, 0.6920 mmol), 5 mL of toluene was placed, to this solution, a mixture of lithium bis(trimethylsilyl)amide (58 mg, 0.3460 mmol) was added and the resulting reaction mixture was kept under stirring at room temperature for 6 hours after that Indium chloride (76 mg, 0.340 mmol) was added into the reaction mixture, kept under stirring for overnight in room temperature then the white precipitate was observed which was filtered off and the to this filtrate, AgOTf (87 mg, 0.340 mmol) was added and the reaction mixture was stirred 30 minutes. The white precipitate of AgCl was filtered off and the filtrate was evaporated under *vacuo* to give a colorless residue. The residue was washed with 5 mL of *n*-pentane. The complex **3a** was re-crystallised from toluene at –35 ºC, and colorless crystals were obtained after 3 days.

Yield: 392 mg, 76%. ^{1}H NMR (400 MHz, C_6D_6, 25 °C): δ_H 7.07 – 7.01 (m, 4H, Ar), 6.96 – 6.90 (m, 2H, Ar), 4.63 (s, 2H, NC*H*), 3.49 – 3.43 (m, 1H, C*H*), 3.07 – 3.00 (m, 1H, C*H*), 1.52 – 1.50 (s, 3H, CH_3), 1.31 (s, 3H, CH_3), 1.25 (s,3H, CH_3) 1.14 – 1.13 (d, 3H, (CH_3)$_2$) 1.05 – 1.02 (d, 3H, (CH_3)$_2$) ppm. ^{13}C{^{1}H} NMR (100 MHz, C_6D_6): δ_C 186.6, 177.4, 143.8, 143.8, 141.6, 137.7, 129.1, 128.4, 127.9, 127.6, 126.4, 125.5, 124.4, 123.0, 97.2, 28.4, 28.2, 26.8, 25.0, 24.8, 24.6, 23.8, 21.2. ppm. ^{19}F{^{1}H} NMR (376.46 MHz, C_6D_6): 76.93 ppm Elemental analysis: $C_{29}H_{36}F_3InN_2O_5S$ (696.5): calcd C 50.01, H 5.21, N 4.02. Found C 49.91, H 5.09, N 3.89.

General procedure for aminophosphorilation reaction by using indium complex as a catalyst:

Inside the glove box to a 25 mL dry Schlenk flask, the required aldehyde precursor (0.9433 mmol, 1 equiv) was added to the reaction mixture of amine (0.9433 mmol, 1 equiv.) and diphenyl phosphine oxide (0.9433 mmol, 1 equiv.) and 2 mol% complex **3a** (18 mg, 0.02358 mmol). The colourless reaction mixture was stirred at room temperature. After 6 hours, the reaction mixture was quenched and workup with water and compound extracted in dichloromethane as an organic layer 3 times. Then the final product was purified by column chromatography in hexane/EtOAc (100:5). The products were identified according to ^{1}H, ^{13}C, and DEPT NMR spectroscopy (wherever necessary), as well as MS analysis.

Conflicts of interest

There are no conflicts to declare.

Acknowledgements

This work was supported by the Science and Engineering Research Board (SERB), Government of India, under project no. (EMR/2016/005150) and Instrumental support provided by Department of Chemistry, IIT Hyderabad. S.D. thanks MHRD and J.B. and A.D. thank UGC India respectively for their Ph.D. fellowships. We also thank Prof. Kazushi Mashima and Prof. Hayato Tsurugi, Osaka University, Japan, for their generous support. PR thanks CSIR for the JRF fellowship. PG acknowledges the Faculty Initiation Grant (FIG–100810) and computational facilities provided by IIT Roorkee.

Notes and references

1 V.P. Kukhar and H.R. Hudson, *Aminophosphonic and Aminophosphinic Acids: Chemistry and Biological Activity, Wiley, Chichester*, 2000.

2 J. Grembecka, A. Mucha, T. Cierpicki and P. J. Kafarski, The Most Potent Organophosphorus Inhibitors of Leucine

Aminopeptidase. Structure-Based Design, Chemistry, and Activity, *Med. Chem.,* 2003, **46**, 2641.
3 W. Liu, C.J. Royers, A.J. Fisher and M.Toney, Aminophosphonate Inhibitors of Dialkylglycine Decarboxylase: Structural Basis for Slow Binding Inhibition, *Biochemistry*, 2002, **41**, 12320.
4 M. Dutartre, J. Bayardon and S. Juge, Applications and stereoselective syntheses of P-chirogenic phosphorus compounds, *Chem. Soc. Rev.* 2016, **45**, 5771-5794.
5 (a) L. Gu and C. Jin, Synthesis and antitumor activity of α-aminophosphonates containing thiazole[5,4-b]pyridine moiety, *Org. Biomol. Chem.* 2012, **10**, 7098-7102; (b) X. C. Huang, M. Wang, Y. M. Pan, G. Y. Yao, H. S. Wang, X. Y. Tian, J. K. Qin and Y. Zhang, Synthesis and antitumor activities of novel thiourea α-aminophosphonates from dehydroabietic acid, *Eur. J. Med. Chem.* 2013, **69**, 508-520; (c) M. Y. Ye, G. Y. Yao, Y. M. Pan, Z. X. Liao, Y. Zhang and H. S. Wang, Synthesis and antitumor activities of novel α-aminophosphonate derivatives containing an alizarin moiety, *Eur. J. Med. Chem.* 2014, **83**, 116-128.
6 (a) N. Ali, S. Zakir, M. Patel and M.Farooqui, Synthesis of new α aminophosphonate system bearing Indazole moiety and their biological activity, *Eur. J. Med. Chem.* 2012, **50**, 39-43; (b) S. Bhagat, P. Shah, S. K. Garg, S. Mishra, P. Kamal Kaur, S. Singh and A. K. Chakraborti, α-Aminophosphonates as novel anti-leishmanial chemotypes: synthesis, biological evaluation, and CoMFA studies, *MedChemComm* 2014, **5**, 665-670.
7 E. K. Fields, The Synthesis of Esters of Substituted Amino Phosphonic Acids, *J. Am. Chem. Soc.* 1952, **74**, 1528-1531.
8 K. Manabe and S. Kobayashi, Facile synthesis of α-amino phosphonates in water using a Lewis acid–surfactant-combined catalyst, *Chem. Commun.* 2000, 669-670.
9 X. J. Mu, M. Y. Lei, J. P. Zou and W. Zhang, Microwave-assisted solvent-free and catalyst-free Kabachnik–Fields reactions for α-amino phosphonates, *Tetrahedron Lett.* 2006, **47**, 1125-1127.
10 D. Pettersen, M. Marcolini, L. Bernardi, F. Fini, R. P. Herrera, V. Sgarzani and A. Ricci, Direct Access to Enantiomerically Enriched α-Amino Phosphonic Acid Derivatives by Organocatalytic Asymmetric Hydrophosphonylation of Imines, *J. Org. Chem.* 2006, **71**, 6269-6272.
11 Z. Y. Zhou, H. Zhang, L. Yao, J. H. Wen, S. Z. Nie and C. Q. Zhao, Double Asymmetric Induction During the Addition of (RP)-Menthyl Phenyl Phosphine Oxide to Chiral Aldimines, *Chirality* 2016, **28**, 132-135.
12 B. Kaboudin and E. Jafari, One-Pot Synthesis of l-Aminophosphinic Acids Using 50% Hypophosphorus Acid under Microwave Irradiation, *J. Iran. Chem. Soc.* 2008, **5**, S97-S102.
13 S. D. Mitragotri, D. M. Pore, U. V. Desai and P. P. Wadgaonkar, ulfamic acid: An efficient and cost-effective solid acid catalyst for the synthesis of α-aminophosphonates at ambient temperature, *Catal. Commun.* 2008, **9**, 1822-1826.
14 S. M. Vahdat, R. Baharfar, M. Tajbakhsh, A. Heydari, S. M. Baghbanian and S. Haksar, Organocatalytic synthesis of α-hydroxy and α-aminophosphonates, *Tetrahedron Lett.* 2008, **49**, 6501-6504.
15 B. Kaboudin and H. Zahedi, Calcium Chloride as an Efficient Lewis Base Catalyst for the One-pot Synthesis of α-Aminophosphonic Esters, *Chem. Lett.* 2008, **37**, 540-541.
16 S. Motevalli, N. Iranpoor, E. Etemadi-Davan and K. R. Moghadam, Exceptional effect of nitro substituent on the phosphonation of imines: the first report on phosphonation of imines to α-iminophosphonates and α-(N-phosphorylamino)phosphonates, *RSC Adv.* 2015**, 5**, 100070-1000076.
17 G. C. S. Reddy, S. Annar, K. U. M. Rao, A. Balakrishna and C. S. Reddy, Synthesis and Anti-microbial activity of a new class of α-Aminophosphonic acid esters by using TMG as Catalyst , *Pharma Chem.* 2010**, 2**, 177-184.
18 S. Bhagat and A. K. Chakraborti, An Extremely Efficient Three-Component Reaction of Aldehydes/Ketones, Amines, and Phosphites (Kabachnik−Fields Reaction) for the Synthesis of α-Aminophosphonates Catalyzed by Magnesium Perchlorate, *J. Org. Chem.* 2007, **72**, 1263-1270.
19 P. Sun, Z. Hu and Z. Huang, Gallium Triiodide Catalyzed Organic Reaction: A Convenient Synthesis of α-Amino Phosphonates, *Synth. Commun.*, 2004, **34**, 4293-4299.
20 H. Firouzabadi, N. Iranpoor and S.Sobhani, Metal Triflate-Catalyzed One-Pot Synthesis of α-Aminophosphonates from Carbonyl Compounds in the Absence of Solvent, *Synthesis*, 2004, 2692-2696.
21 A.K. Bhattacharya and T.Kaur, An Efficient One-Pot Synthesis of α-Amino Phosphonates Catalyzed by Bismuth Nitrate Pentahydrate, *Synlett*, 2007, **5**, 745-748.
22 P. Sun, Z. Hu and Z. Huang, Gallium Triiodide Catalyzed Organic Reaction: A Convenient Synthesis of α-Amino Phosphonates Gallium Triiodide Catalyzed Organic Reaction: A Convenient Synthesis of α-Amino Phosphonates, *Synth. Commun.*, 2004, **34**, 4293-4299.
23 Z. P. Zhan and J. P. Li, Bismuth(III) Chloride–Catalyzed Three-Component Coupling: Synthesis of α-Amino Phosphonates, *Synth. Commun.*, 2005, **35**, 2501-2508.
24 F. Xu, Y. Luo, J. Wu, Q. Shen and H. Chen, Facile one-pot synthesis of α-amino phosphonates using lanthanide chloride as catalyst, *Heteroat. Chem.* 2006, **17**, 389-392.
25 J. Wu, W. Sun, W. Z. Wang and H. G. Xiu, Highly Efficient Catalyst FeCl3 in the Synthesis of α-Amino Phosphonates via Three-component Reactions, *Chinese J. Chem.*, 2006, **24**, 1054-1057.
26 K. Ravinder, A. Vijender Reddy, P. Krishnaiah, G. Venkatara mana, V.L. Niranjan Reddy and Y. Venkateswarlu, CAN Catalyzed One-Pot Synthesis of α-Amino Phosphonates from Carbonyl Compounds, *Synth. Commun.*, 2004, **34**, 1677.
27 (a) B.C. Ranu, A. Hajra and U. Jana, General Procedure for the Synthesis of α-Amino Phosphonates from Aldehydes and Ketones Using Indium(III) Chloride as a Catalyst, *Org. Lett.*, 1999, **1**, 1141-1143; (b) R. Ghosh, S. Maiti, A. Chakraborty, D. K. Maiti, In(OTf)3 catalysed simple one-pot synthesis of α-amino phosphonates, *J Mol Catal A Chem*, 2004, **210**, 53–57.
28 S. Lee, J.H. Park, J. Kang and J.K. Lee, Lanthanide triflate-catalyzed three component synthesis of α-amino phosphonates in ionic liquids. A catalyst reactivity and reusability study, *Chem. Commun.*, 2001, 1698-1699.
29 a) K. Ramakrishna, J. M. Thomas, and C. Sivasankar, A Green Approach to the Synthesis of α-Amino Phosphonate in Water Medium: Carbene Insertion into the N–H Bond by Cu(I) Catalyst, *J. Org. Chem.* 2016, **81**, 9826–9835; (b) Y. Q. Yu, An Efficient and Convenient Procedure for the One-Pot Synthesis of α-Aminophosphonates from Aryl Azides under Solvent-Free Conditions, *Synthesis* 2013, **45**, 2545-2550.
30 G. D. Joly and E. N. Jacobsen, Thiourea-Catalyzed Enantioselective Hydrophosphonylation of Imines: Practical Access to Enantiomerically Enriched α-Amino Phosphonic Acids, *J. Am. Chem. Soc.* 2004, **126**, 13, 4102-4103.
31 J.S. Yadav, B.V.S. Reddy and P. Sreedhar, n eco-friendly approach for the synthesis of α-aminophosphonates using ionic liquids, *Green Chem.,* 2002, **4**, 436-438.
32 S. Lee, J.K. Lee, C.E. Song and D. C. Kim, Microwave-assisted Kabachnik-Fields Reaction in Ionic Liquid Sang-gi Lee, Jae Kyun Lee, Choong Eui Song and Dok-Chan Kim, *Bull. Korean Chem. Soc.,* 2002, **23**, 667-668.
33 M. M. Kabachnik, E. V. Zobnina and I. P. Beletskaya, Microwave-Assisted Reactions of Schiff Bases with Diethyl Phosphonate in the Presence of CdI2, *Russ. J. Org. Chem.* 2005**, 41**, 505-507.
34 B. H. Alexander, L. S. Hafner, M. V. Garrison and J. E. Brown, Another Example of the Novel Conversion of a Phosphonate to a Phosphate, *J. Org. Chem.* 1963**, 28**, 3499-3501.

35 X. H. Liu, J. Q. Weng, C. X. Tan, L. Pan, B. L. Wang and Z. M.Li, Synthesis, Biological Activities and DFT Calculation of a-Aminophosphonate Containing Cyclopropane Moiety, *Asian J. Chem.* 2011**, 23***,* 4031-4036.
36 A. C. Gaumont, A. Simon and J. M. Denis, Uncatalyzed hydrophosphination of multiple bonds by alkenyl or alkynylphosphine oxides; evidence for a P-H activation, *Tetrahedron* 1998**, 39***,* 985-988.
37 C. Hoarau, A. Couture, E. Deniau and P.Grandclaudon, A New Synthetic Approach to Dioxoaporphines 2 Application to the Synthesis of N-Methylouregidione, *Eur. J. Org. Chem.* 2001**,** 2559-2567.
38 G. K. Ingle, Y. Liang, M. G. Mormino, G. Li, F. R. Fronczek and J. C. Antilla, Chiral Magnesium BINOL Phosphate-Catalyzed Phosphination of Imines: Access to Enantioenriched α-Amino Phosphine Oxides, *Org. Lett.* 2011**, 13***,* 2054-2057.
39 T. P. Loh, J. Pei and M.Lin, Indium trichloride (InCl3) catalyzed Diels–Alder reaction in water, *Chem. Commun.* 1996, 2315-2016.
40 T. P. Loh, J. Pei and G. Q. Cao, Indium trichloride catalyzed Mukaiyama aldol reaction in water *Chem. Commun.* 1996, 1819-1820.
41 B. C. Ranu and U. Jana, Indium (III) chloride-promoted rearrangement of epoxides: A selective synthesis of substituted benzylic aldehydes and ketones, *J. Org. Chem.* 1998, **63**, 8212-8216.
42 T. Miyai, Y. Onishi and A. Baba, Indium trichloride catalyzed reductive Friedel-Crafts alkylation of aromatics using carbonyl compounds, *Tetrahedron Lett.* 1998, **39**, 6291-6294.
43 A. N. Tishkina, A. N. Lukoyanov, A. G. Morozov, G. K. Fukin, K. A. Lyssenko and I. L. Fedushkin, Synthesis and structure of novel chiral amido-imine complexes of aluminum, gallium, and indium, *Russ Chem Bull*, 2009*,* **58**, 2250-2257.
44 F. Neese, The ORCA program system, *WIREs Comput. Mol. Sci.* 2012, **2**, 73−78.
45 J. P. Perdew, Density-functional approximation for the correlation energy of the inhomogeneous electron gas, *Phys. Rev. B* 1986, **33**, 8822–8824.
46 A. D. Becke, Density-functional exchange-energy approximation with correct asymptotic behavior, *Phys. Rev. A* 1988, **38**, 3098–3100.
47 S. Grimme, S. Ehrlich, L. Goerigk, Effect of the damping function in dispersion corrected density functional theory, *J. Comput. Chem.* 2011, **32**, 1456–1465.
48 F. Weigend, R. Ahlrichs, Balanced basis sets of split valence, triple zeta valence and quadruple zeta valence quality for H to Rn: Design and assessment of accuracy, *Phys. Chem. Chem. Phys.* 2005, **7**, 3297–3305.
49 F. Neese, Importance of Direct Spin−Spin Coupling and Spin-Flip Excitations for the Zero-Field Splittings of Transition Metal Complexes: A Case Study, *J. Am. Chem. Soc.* 2006, **128**, 10213–10222.
50 S. Das, R. Kumar, A. Devadkar and T. K. Panda, Zinc Complexes of β-Ketoiminato Ligands as Efficient Catalysts for the Synthesis of α-Amino Nitriles via Strecker Reaction, *Asian J. Org. Chem.,* 2020, **9**, 1217-1224.